

# 1 Direct RNA nanopore sequencing of SARS-CoV-2 extracted 2 from critical material from swabs

3  
4 **Davide Vacca<sup>at</sup>, Antonino Fiannaca<sup>bt</sup>, Fabio Tramuto<sup>a</sup>, Valeria Cancila<sup>a</sup>, Laura La Paglia<sup>b</sup>,  
5 Walter Mazzucco<sup>a</sup>, Alessandro Gulino<sup>c</sup>, Massimo La Rosa<sup>b</sup>, Carmelo Massimo Maida<sup>a</sup>,  
6 Gaia Morello<sup>a</sup>, Beatrice Belmonte<sup>a</sup>, Alessandra Casuccio<sup>a</sup>, Rosario Maugeri<sup>d</sup>, Gerardo  
7 Iacopino<sup>d</sup>, Francesco Vitale<sup>as</sup>, Claudio Tripodo<sup>as</sup>, Alfonso Urso<sup>bs</sup>**

8  
9 <sup>a</sup> University of Palermo, Department of Sciences for Health Promotion and Mother-Child Care  
10 “G. D’Alessandro”, Piazza delle cliniche N°2, zip code 90127, Palermo, Italy.

11  
12 <sup>b</sup> CNR-ICAR, National Research Council of Italy, Via Ugo La Malfa, a5c, Palermo, Italy.

13  
14 <sup>c</sup> Cogentech srl Società Benefit, FIRC Institute of Molecular Oncology (IFOM)  
15 Via Adamello 16, 20139, Milan, Italy

16  
17 <sup>d</sup> Department of Experimental Biomedicine and Clinical Neurosciences, School of Medicine,  
18 Neurosurgical Clinic, University of Palermo, Palermo, Italy.

19  
20 <sup>†</sup> Equal contributors.

21 <sup>§</sup> Equal contributors

## 22 23 **ABSTRACT**

24 **Background.** In consideration of the increasing prevalence of COVID-19 cases in  
25 several countries and the resulting demand for unbiased sequencing approaches, we  
26 performed a direct RNA sequencing experiment using critical oropharyngeal swab  
27 samples collected from Italian patients infected with SARS-CoV-2 from the Palermo  
28 region in Sicily.

29 **Methods.** Here, we identified the sequences SARS-CoV-2 directly in RNA extracted  
30 from critical samples using the Oxford Nanopore MinION technology without prior cDNA  
31 retro-transcription.

32 **Results.** Using an appropriate bioinformatics pipeline, we could identify mutations in the  
33 nucleocapsid (N) gene, which have been reported previously in studies conducted in  
34 other countries.

35 **Conclusion.** To the best of our knowledge, the technique used in this study has not  
36 been used for SARS-CoV-2 detection previously owing to the difficulties in the  
37 extraction of RNA of sufficient quantity and quality from routine oropharyngeal swabs.

38 Despite these limitations, this approach provides the advantages of true native RNA  
39 sequencing, and does not include amplification steps that could introduce systematic  
40 errors.

41 This study can provide novel information relevant to the current strategies adopted in  
42 SARS-CoV-2 next-generation sequencing.

43 We deposited the gene sequence in the NCBI database under the following  
44 URL:<https://www.ncbi.nlm.nih.gov/nucleotide/MT457389>

45

46 **KEYWORDS** MinION, Direct RNA Nanopore sequencing, Sars-CoV-2, Covid19, Swab

47

## 48 **INTRODUCTION**

49 The study of the SARS-CoV-2 genome has become a priority for global healthcare to  
50 facilitate the identification of more suitable vaccines and therapeutic drugs (1).

51 The use of third generation sequencing technologies has increased significantly in  
52 recent years, as these methods yield reliably long reads even from biological samples  
53 with noise (2).

54 Direct RNA sequencing (RNA-seq) of SARS-CoV-2 has the advantage of displaying its  
55 native sequence without contamination by artefacts originating from the in vitro cDNA  
56 amplification step, which is often necessary for target enrichment (3). However, the  
57 quality of RNA extracted from the swab has certain critical issues with respect to both  
58 fragmentation level and concentration, such that the read coverage of sequencing  
59 decreases considerably. In this study, we investigate the suitability of Nanopore Oxford  
60 MinION Mk1B (4), a third-generation nanopore-based platform, for the identification of a  
61 critical target of SARS-CoV-2 native RNA from a swab sample, and its sensitivity in the  
62 characterization of the viral mutational landscape.

63 To this end, we analyzed ten RNA samples extracted from oropharyngeal swabs of ten  
64 patients with COVID-19, and sequenced them in two pools following the direct RNA  
65 sequencing protocol (SQK-RNA002, Nanopore Technologies). Although the  
66 concentration of the library loaded in the sequencing flow cell was approximately 200  
67 times lower than that required for the protocol, we clearly identified two mutations in the  
68 nucleocapsid phosphoprotein (N) gene with respect to the sequence of the strain  
69 isolated in Wuhan, which has been described in literature.

70

## 71 **MATERIALS AND METHODS**

72 After the collection of ten oropharyngeal swab samples from Italian patients with  
73 COVID-19, we assayed the concentration and fragmentation level of the extracted RNA  
74 to arrange it for sequencing, as recommended by Oxford Nanopore in the Input  
75 DNA/RNA quality control guidelines (5). Next, we prepared two sequencing libraries  
76 from two distinct pools, as described below, and launched a computational pipeline for

77 aligning the obtained reads. Lastly, we confirmed the mutation frequency in our sample  
78 either by Sanger sequencing or by real-time PCR (qPCR) assays.

79

## 80 **Input RNA collection and quality control steps**

81

82 **Samples.** For this study, we collected RNA samples from ten Sicilian patients between  
83 March 19<sup>th</sup> and 23<sup>rd</sup>, 2020. The patients tested positive in the 2019-Novel Coronavirus  
84 (2019-nCoV) Real-time rRT-PCR Panel (Centers for Disease Control and Prevention  
85 (CDC) Atlanta, GA 30333).

86 Furthermore, to compare the nanopore sequencing results, we included two samples  
87 from uninfected individuals as negative controls. The RNA from uninfected controls was  
88 extracted from brain biopsy specimens of two patients who underwent surgery in August  
89 2019 and in January 2020, respectively. Both biopsies were made available from  
90 Department of Experimental Biomedicine and Clinical Neurosciences, School of  
91 Medicine, Neurosurgical Clinic, University of Palermo.

92

93 **RNA extraction.** The swab buffer kit was assayed using the QIAamp Viral RNA Mini Kit  
94 in Automated purification of RNA on QIAcube Instruments (Qiagen, Cat.No 9001292)  
95 according to the manufacturer's instructions.

96

97 **Assessment of concentration and fragmentation level.** The quality of the  
98 fragmented sample was assessed with an Agilent Bioanalyzer 2100 (Agilent, Cat.No  
99 G2939BA) using the Agilent RNA 6000 Pico assay (Agilent, Cat.No 5067-1513). We  
100 assayed 1  $\mu$ L of each pure sample. The RNA extracted from the samples showed high  
101 fragmentation and lowest concentration levels with an RIN index between 2.6 and 2.1  
102 and concentration between 19 and 829  $\text{pg}/\mu\text{L}$ .

103

## 104 **Preparation of the libraries and the computational pipeline**

105 The samples were organized in two pools (A and B), each with a final volume of 10  $\mu\text{L}$ .  
106 Pool A included samples from three patients: two with a PCR cycle threshold (Ct) value  
107 of 18 and one with Ct value of 20. To elaborate, we pooled 8  $\mu\text{L}$  of samples from the  
108 first two patients (4  $\mu\text{L}$  from each) and 2  $\mu\text{L}$  from the last patient.

109 Pool B included RNA samples collected from ten patients (1  $\mu\text{L}$  from each patient):  
110 three samples were from pool A, while the other seven had decreasing Ct values, and  
111 were collected from two patients with Ct value of 21, two with 22, two with 23, and one  
112 with 24.

113 **Library preparation, priming, and commencement of a sequencing run.** Both pools  
114 were sequenced using a MinION Mk1B sequencer with the SQK-RNA002 protocol.

115 After preparing the sequencing libraries A and B, as previously described, to ligate  
116 retro-transcription adapters (RTA) to the 3'-end of the RNA molecules, we combined  
117 each library with 6  $\mu\text{L}$  of a mix comprising 3  $\mu\text{L}$  of NebNext Quick Ligation Reaction  
118 Buffer, 1.5  $\mu\text{L}$  of T4 DNA Ligase, 1  $\mu\text{L}$  of RTA, and 0.5  $\mu\text{L}$  of 110 nM RNA CS (RCS).  
119 Each reaction was incubated for 10 min at 22  $^{\circ}\text{C}$ . Next, the reactants were mixed with 9  
120  $\mu\text{L}$  of nuclease-free water, 8  $\mu\text{L}$  of 5X first-strand buffer, 4  $\mu\text{L}$  of 0.1 DTT, and 2  $\mu\text{L}$  of 10  
121 mM dNTPs. For cDNA synthesis, we added 2  $\mu\text{L}$  of SuperScript III, following which both  
122 reactions were incubated under the following conditions: 50  $^{\circ}\text{C}$  for 50 min, 70  $^{\circ}\text{C}$  for 10  
123 min, and 4  $^{\circ}\text{C}$  before proceeding to the next step.

124 The subsequent wash step was performed according to the procedure for the specified  
125 protocol.

126 Next, we measured the concentration of 1  $\mu\text{L}$  of each library using a Qubit 3.0  
127 Fluorimeter and the dsDNA HS assay kit (Life Technologies, Cat. No Q32851). The  
128 concentrations were 1.2 ng/ $\mu\text{L}$  and 0.6 ng/ $\mu\text{L}$  for libraries A and B, respectively.

129 Next, we performed the Attachment of 1D sequencing adapter step according to  
130 manufacturer instructions, and recorded final concentrations of 0.9 ng/ $\mu\text{L}$  and 0.3 ng/ $\mu\text{L}$   
131 for A and B, respectively.

132 Lastly, 20  $\mu\text{L}$  of sample from each library was mixed with 17.5  $\mu\text{L}$  of nuclease-free water  
133 and 37.5  $\mu\text{L}$  of RNA running buffer (RRB) in a final volume of 75  $\mu\text{L}$ .

134 The assessment of the R9.4 Flow Cell, which was performed prior to the loading of the  
135 libraries, revealed that 1575 active pores were available for sequencing.

136 We performed a new MinKNOW (6) (*v19.12.5*) experiment using only the A loading mix  
137 in the flow cell.

138 In MinKNOW we selected the SQK-RNA002 Kit and continued the sequencing process  
139 until approximately 80% pores were available (i.e., after 4 h). At this point, we paused  
140 the process and loaded the B loading mix in the flow cell. Next, the run was resumed  
141 and continued till the number of reads generated was unvaried at 397k (i.e., after  
142 approximately 27 h). At the end of the sequencing process, we obtained the "Fast5" raw  
143 data files.

144  
145 **Computational pipeline.** We developed a computational pipeline to analyze the output  
146 from the Oxford Nanopore MinION device. The first step in the process involved the  
147 conversion of "Fast5" in "Fastq" format. For this, we used the GPU version of the  
148 Nanopore *Guppy* basecaller (*v3.4.4*) tool (7) with the following parameters: "*flow\_cell =*  
149 *FLO-MIN106*" and "*kit = SQK-RNA002*".

150 As a second step, we performed read quality control using the *PycoQC* (*v2.5.0.21*)  
151 software (8) with standard parameters. This tool computes metrics and generates  
152 multiple quality plots for Nanopore technologies that allow the initial evaluation of the  
153 sequenced reads.

154 *PycoQC* can subsequently provide an overview of the overall quality of the reads. To  
155 clean the input data, we filtered the quality and read length using the *NanoFilt* (v2.7.0)  
156 tool (9). This tool can also analyze the sequencing summary file generated by  
157 *guppy\_basecaller* to refine the filtering process. For these reasons, we filtered the reads  
158 using the sequencing summary file under the following parameters: minimum read  
159 length  $\geq 500$  nt and read quality  $\geq 8$ .

160 Thereafter, only the filtered reads were considered in further analysis.

161 At this point, we created an alignment process that mapped reads to a reference  
162 genome and identified the exact genomic loci corresponding to each read. Given that,  
163 we did not use primers for the amplification of the SARS-CoV-2 genome, we had to  
164 remove all the reads that were mapped with other material sequenced from the swabs.  
165 In this study, to remove the contaminating sequences, we considered humans, fungal,  
166 and bacterial reference genomes, respectively. To elaborate, we used the "Homo  
167 sapiens genome assembly *GRCh38 (hg38)*" from the Genome Reference Consortium  
168 (10) as the human reference genome, and all sequences from both fungal and bacterial  
169 genome projects from NCBI (11). Lastly, we used the NCBI SARS-CoV-2 sequence  
170 NC\_045512.2 (12) as a reference genome for SARS-CoV-2.

171 For each of these reference genomes, we mapped the reads using the *minimap2*  
172 (v2.17-r941) tool (13) based on earlier reports that demonstrated the effective  
173 performance of this tool with the splice-aware alignment of Nanopore Direct RNA reads  
174 against a reference genome (14). As suggested by authors who reported the  
175 performance of *minimap2*, we set the parameter  $k = 13$  to increase the sensitivity and to  
176 map noisy Nanopore Direct RNA-seq reads.

177 Next, we extracted both unmapped reads and reads with mapping quality lower than 10  
178 using the "view" utility in the *samtools* (v1.7) library (15) for each reference genome  
179 except for that of SARS-CoV-2.

180 Resultantly, we obtained a sub-set of the sequenced long-reads that did not map with  
181 the genomes of human, fungi, or bacteria.

182 Lastly, we mapped the remaining reads against the SARS-CoV-2 reference genome  
183 using *minimap2* tools with the same parameters used earlier. We successively analyzed  
184 the results of the mapping process using the *BCFtools* (v1.9) library (16), a set of  
185 utilities for variant calling. In particular, we first used the *mpileup* tool (16) to generate a  
186 summary of the coverage of the mapped reads on the SARS-CoV-2 reference genome  
187 at single base-pair resolution, followed by the *call* tool (17) for generating calls. We set  
188 these tools to perform as the standard consensus-caller with only the variant sites  
189 returned. The results of this pipeline were enlisted as SARS-CoV-2 variants detected in  
190 the sequenced samples from the swabs.

191

192

## 193 **Calculation of mutation frequency**

194

195 **Sanger sequencing.** The samples were sequenced using the BigDye™ Terminator  
196 v3.1 Cycle Sequencing Kit (Life Technologies; Cat no 4337455) with an ABI PRISM  
197 3100 Genetic Analyzer upgraded to the Applied Biosystems® 3130xl System (Life  
198 Technologies; Cat no 4359571). To enrich the identified mutation region in the N gene,  
199 we adopted a nested PCR approach using an outer and an inner primer sets. Both  
200 primer sets are reported in Tab. S1.

201

202 **RT-PCR.** The ten sequenced samples and the two uninfected control RNAs were retro-  
203 transcribed using the EcxcelRT™ Reverse Transcription kit (SMOBIO, Cat. No RP1300).  
204 First, 16 µL of each sample was mixed with 2 µL of 50 µM of Oligo (dT)<sub>20</sub> primer and 2  
205 µL of dNTP Mix (10 mM each). The mixes were incubated at 70 °C for 5 min and placed  
206 on ice for at least 1 min. Next, 8 µL of 5X RT Buffer (DTT), 8 µL of DEPC-Treated water,  
207 2 µL of RNAok™ Rnase Inhibitor, and 2 µL ExcelRT™ Reverse Transcriptase was  
208 added to each sample. The reactions were incubated at 25 °C for 10 min, at 44 °C for  
209 50 min, and at 85 °C for 5 min, and were subsequently held at 4 °C.

210

211 **qPCR.** To amplify the region containing the NC\_045512:c.608\_609\_610delinsAAC  
212 mutation, we designed two primer sets to distinguish between a wild type (WT) and a  
213 mutated viral strain. The two sets used the same reverse primer, with divergence at the  
214 last three bases at the 3'-end of the forward primer. In fact, one forward primer was  
215 specific for the mutated sequence, whereas the other recognized the reference  
216 sequence.

217 We used two other sets as controls. One set consisted of the primers N2 from the 2019-  
218 Novel Coronavirus (2019-nCoV) Real-time rRT-PCR Panel (Centers for Disease Control  
219 and Prevention (CDC) Atlanta, GA 30333), which was used to confirm the presence of  
220 the N gene target (Fig. S1 and Tab. S2). The second set consisted of a custom specific  
221 primer for human *GAPDH* cDNA, which was used as an endogen control for the PCR  
222 (Fig. S2 and Tab. S3). All primer sequences are listed in Tab. S1.

223 Moreover, a plasmid vector carrying a synthetic reference SARS-CoV-2 N gene  
224 (Origene, Cat No: VC202563) was used as a reference control.

225 First, both analysis samples and uninfected control cDNA samples were diluted at a 1:2  
226 ratio, while the reference control was concentrated to 0.8 ng/µL. Next, 4 µL of each  
227 sample in 20 µL of reaction mixture was assayed by qPCR using the Quantinova SYBR  
228 Green PCR kit (Qiagen, Cat No.: 208052) according to the manufacturer's instructions  
229 in a Rotor-Gene Q 5plex HRM Thermocycler (Qiagen, Cat No./ID: 9001580). The  
230 following PCR thermal profile was used: 95 °C, 2 min; 95 °C, 5 s and 57 °C, 10 s for 35  
231 cycles.

232

233

## 234 RESULTS

235 To characterize the SARS-CoV-2 mutational landscape, we used RNA extracted from  
236 samples collected from five male and five female patients who tested positive for SARS-  
237 CoV-2 in the swab-test, with the corresponding Ct values ranging from 18 to 24. First,  
238 we assessed the concentrations and the fragmentation levels in the samples, as  
239 reported in the Materials and Methods. The overall samples had significantly low  
240 concentrations (in the order of pg/ $\mu$ L) and high fragmentation levels with an RIN index  
241 ranging from 2.6 to 2.1. Next, we prepared the pools A and B from the samples, as  
242 explained in the Materials and Methods. We prepared the former to increase the  
243 abundance of sequencing output and the latter to improve the heterogeneity in the data.  
244 We set up each pool at a final volume of 10  $\mu$ L, and prepared the libraries for direct  
245 RNA-seq, as described in the Materials and Methods.

246 After each purification step, the concentrations were 1.2 ng/ $\mu$ L and 0.6 ng/ $\mu$ L in the  
247 initial eluates, and 0.9 ng/ $\mu$ L and 0.3 ng/ $\mu$ L in the final eluates at the pre-sequencing  
248 stage for pools A and B, respectively.

249 Although the library concentrations were 200 times less than that required for the  
250 protocol, we opted to load the libraries and test the suitability of MinION.

251 To perform a single MinION sequencing run, we loaded library A in the flow cell at the  
252 beginning of the run with 1,575 active pores enabled, while library B was loaded when  
253 1,260 active pores remained active, as described in the Materials and Methods.

254 Using the *MinKNOW* and *Guppy* basecaller tools, we obtained a set of 397,465 reads in  
255 the Fastq format file.

256 As we stated previously, the overall quality of reads is affected by the adopted  
257 sequencing technique; i.e., the direct RNA sequencing of samples derived from the  
258 swabs. In this experiment, the average read length was lower than that of standard  
259 long-reads, and the quality of certain reads was below conventional levels. Therefore,  
260 we preferred to discard the reads that had low quality ( $< 8$ ) as well as a short length ( $<$   
261 500 nt). We obtained a subset of 20,940 good-quality reads.

262 At this point, we aimed to identify and remove sequences from contaminant species  
263 contained in the swab; for this, we used the *minimap2* tool (13) to filter out reads that  
264 mapped with sequences from human, fungal, and bacterial genomes.

265 Using this method, we filtered 97.63% of the reads; details of the composition of these  
266 reads are provided in Tab. S4. Lastly, we attempted to map the remaining 2.37% of  
267 reads with the SARS-CoV-2 reference genome, and observed that 10.89% of the reads  
268 (i.e., 54 reads) mapped. These reads did not cover the entire SARS-CoV-2 reference  
269 genome; however, these were sufficient for mapping the N gene.



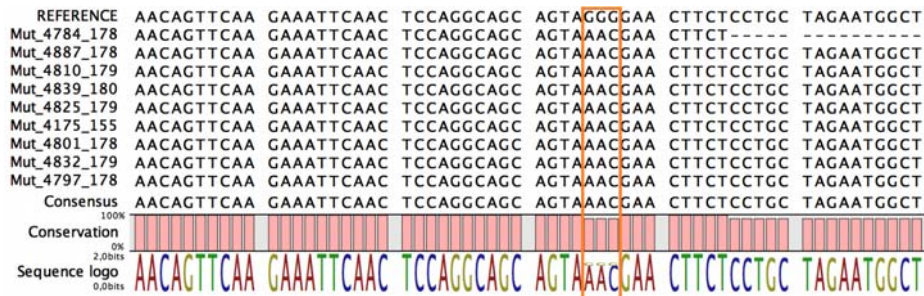


**Fig. 2** The sequences obtained by Sanger sequencing of RNA extracted from swabs who tested positive for SARS-CoV-2 infection. The rectangle covers coordinates from 28881 to 28883 for underlines as all samples contained the NC\_045512:c.28881\_28882\_28883delinsAAC mutation.

In the qPCR assay, we used custom primer sets designed to distinguish between WT and mutated sequences, and another pair set, as reported in the Materials and Methods. We compared two uninfected controls and the synthetic SARS-CoV-2 N cDNA, which was similar to the reference control. All the samples yielded positive results with the primer set specified for the mutated sequence (Fig. S3 and Tab. S5) and negative for the WT sequence (Fig. S4 and Tab. S6), in contrast to that for the reference control, consistent with the results of the Sanger sequencing experiment. The uninfected samples tested negative for both mutated and WT sets, which confirmed the absence of a possible off-target from the host.

## DISCUSSION

Next-generation sequencing technologies can be used to detect the nucleotide sequences in analyzed samples within a short duration and at an affordable cost (18). However, these approaches depend on both the harvest and extraction protocols of the sample, which significantly influence the coverage and depth of the sequencing reads (21, 22).

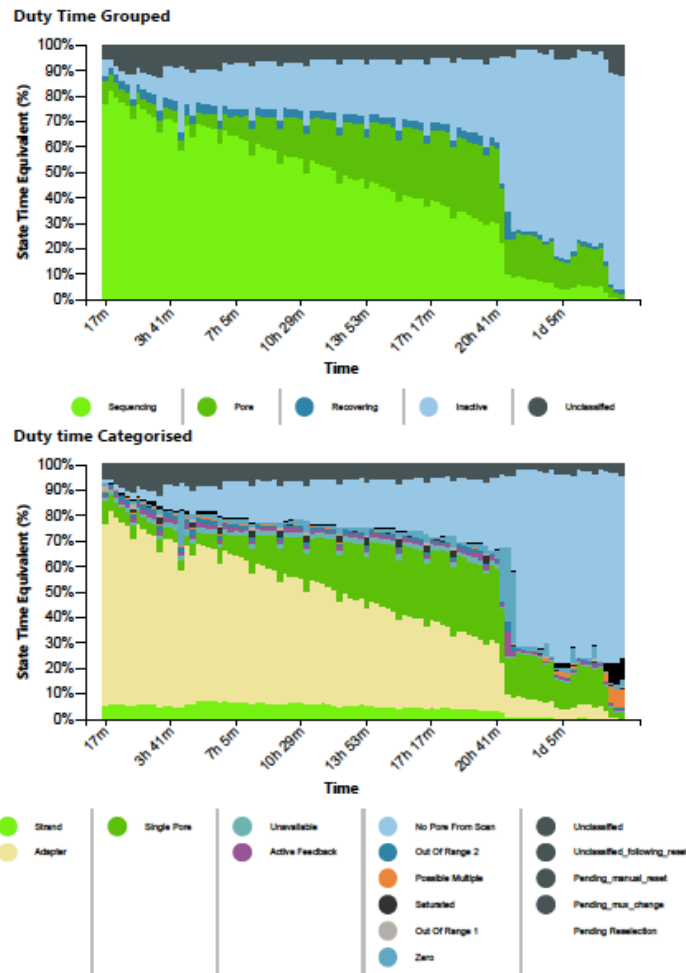
Even though cDNA sequencing is considered the gold standard for the analysis of critical materials (23), DNA polymerase can introduce certain read errors during the DNA synthesis step, which can considerably affect the SNPs analysis (3, 22).

Instead, direct RNA-seq can help identify the native sequences without contamination by artefacts that are usually introduced in the in vitro amplification step, even though it requires a higher input concentration compared to cDNA sequencing methods (21)

In this context, swab RNA, which has a lower concentration and is also more fragmented than in vitro RNA, may not be suitable for performing direct sequencing.

However, the performance of the MinION flow cell has improved exponentially in recent years (2); therefore, we chose to utilize MinION Mk1B to characterize the mutational landscape in the critical samples.

325 To maintain the sequencing input concentration and its heterogeneity, we combined  
326 RNA samples from two pools (A and B). At the end of the library workflow, both samples  
327 were present at concentrations that were approximately 200 times less than that  
328 required for the protocol. In fact, owing to insufficient starting material, we observed that  
329 only a limited number of pores were active at a time, as shown in the MinKNOW duty  
330 time plot in Fig. 3.

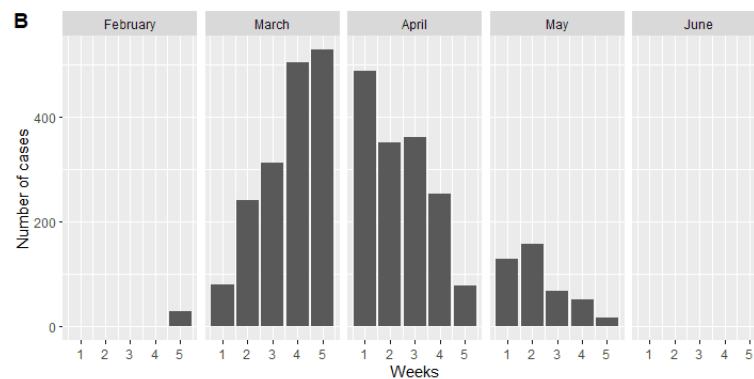
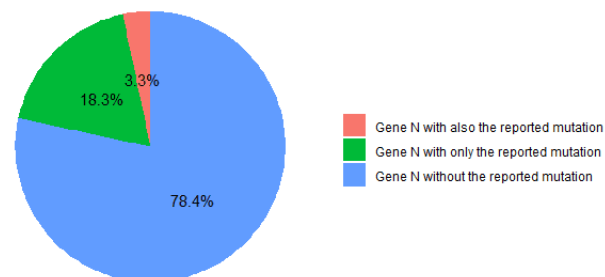


331  
332 **Fig. 3** The MinKNOW duty time plots depict the sum of total channel activity within a  
333 particular period of time. The number of sequencing pores decrease over time. In the  
334 categorized plot, the imbalance of adapters is apparent.

335  
336 Resultantly, we only obtained a few reads (approximately 0.3%), which showed  
337 significant variant calling. Next, we investigated whether findings from other studies on  
338 SARS-CoV-2 were consistent with our findings. To this end, we considered sequence  
339 variations from the China National Center for Bioinformatics (CNGB) portal (23). CNGB  
340 is the largest, daily-updated, publicly available SARS-CoV-2 genome variation  
341 repository. It contains more than 21,000 high-quality, human-hosted, complete SARS-  
342 CoV-2 genomes (last download on 12-Jun-2020) from several countries worldwide. We

343 retrieved this dataset and prepared a script to check for the presence of the identified  
344 mutation region (NC\_045512:c.28881\_28882\_28883delinsAAC) in the sequences of N  
345 gene present in CNCB's dataset. As shown in Fig. 4A, we considered three sets: 1)  
346 cases that only contained identified mutations, 2) cases that also contained identified  
347 mutations, and 3) cases that did not contain the identified mutations. We found that the  
348 same N gene sequence reported by us was reported in approximately 18% of COVID-  
349 19 cases, and we took into account the distribution of these cases over time.  
350 As shown in Fig. 4B, we reported the presence of the mutation in cases treated per  
351 week from February to June, and noticed that the majority of cases were reported  
352 between the second week of March and the fourth week of April. This period coincided  
353 with that of swab collection from patients.

A Distribution of the reported mutation in CNCB



354 **Fig. 4** Identification of the reported mutation in the CNCB database. (A) Strains  
355 isolated from 18.3% of COVID-19 cases (over 21,000 complete genomes sequenced  
356 from isolated strains) contained the reported mutation. (B) Plot depicting the  
357 distribution of these cases from the end of February to the beginning of June.  
358  
359

360 Lastly, we wanted to compare the in silico results using Sanger sequencing and qPCR  
361 techniques, as described in the Results section. The presence of the  
362 NC\_045512:c.28881\_28882\_28883delinsAAC mutation was confirmed using both  
363 methods in all the samples used in this study. Our results validated the approach of  
364 direct RNA-seq with Oxford Nanopore MinION technology. Additionally, the presence of

365 molecular targets for the identification of specific genomic mutations was confirmed, and  
366 could be considered advantageous for both surveillance and epidemiologic studies.

367

### 368 **Data availability**

369 The data that support the findings of this study are available from the corresponding  
370 author upon reasonable request.

371 Supplemental material is available to link:

372 [https://www.dropbox.com/sh/yphu9kzd64mnrI7/AAC8khoPjZ8wSeZRk\\_6DFd6a?dl=](https://www.dropbox.com/sh/yphu9kzd64mnrI7/AAC8khoPjZ8wSeZRk_6DFd6a?dl=0)  
373 0

374

### 375 **Contributions**

376 DV: Data curation, Formal analysis, Methodology, Software, Writing, Editing; AF: Data  
377 curation, Formal analysis, Methodology, Software, Writing, Editing; FT: Investigation,  
378 Methodology, Resources, Visualization; VC: Investigation, Methodology, Visualization;  
379 LLP: Visualization, Review, Editing; WM: Investigation, Resources, Visualization; AG:  
380 Data curation, Visualization; MLR: Data curation, Methodology, Visualization, Review,  
381 Editing; CM: Data curation, Methodology, Resources, Visualization; GM: Data curation,  
382 Methodology, Visualization; BB: Data curation, Visualization; AC: Data curation,  
383 Investigation, Resources, Visualization; RM: Resources, Visualization; GI: Resources,  
384 Visualization; FV: Conceptualization, Data curation, Investigation, Supervision,  
385 Visualization, Writing, Review, Editing; CT: Conceptualization, Data curation, Funding  
386 acquisition, Investigation, Project administration, Supervision, Visualization, Writing,  
387 Review, Editing; AU: Conceptualization, Data curation, Investigation, Supervision,  
388 Visualization, Writing, Review, Editing

389

### 390 **Conflicts of interest.**

391 All authors no reported conflicts.

392

### 393 REFERENCES

- 394 1. Bafna K, Krug RM, Montelione GT. Structural Similarity of SARS-CoV2 Mpro and HCV  
395 NS3/4A Proteases Suggests New Approaches for Identifying Existing Drugs Useful as  
396 COVID-19 Therapeutics. Preprint. ChemRxiv. 2020;10.26434/chemrxiv.12153615.v1.  
397 Published 2020 Apr 21. doi:10.26434/chemrxiv.12153615
- 398 2. Kono N, Arakawa K. Nanopore sequencing: Review of potential applications in functional  
399 genomics. Dev Growth Differ. 2019;61(5):316-326. doi:10.1111/dgd.12608
- 400 3. Brandariz-Fontes C, Camacho-Sanchez M, Vilà C, Vega-Pla JL, Rico C, Leonard JA. Effect  
401 of the enzyme and PCR conditions on the quality of high-throughput DNA sequencing  
402 results. Sci Rep. 2015;5:8056. Published 2015 Jan 27. doi:10.1038/srep08056; Depledge

- 403 DP, Wilson AC. Using Direct RNA Nanopore Sequencing to Deconvolute Viral  
404 Transcriptomes. *Curr Protoc Microbiol.* 2020;57(1):e99. doi:10.1002/cpmc.99
- 405 4. Oxford Nanopore Technologies, Nanopore Oxford MinION 1kb,  
406 [https://community.nanoporetech.com/requirements\\_documents/minion-it-reqs.pdf](https://community.nanoporetech.com/requirements_documents/minion-it-reqs.pdf)
- 407 5. Oxford Nanopore Technologies, Input DNA/RNA QN,  
408 <https://community.nanoporetech.com/protocols/input-dna-rna->  
409 [qc/v/IDI\\_S1006\\_v1\\_revB\\_18Apr2016](https://community.nanoporetech.com/protocols/input-dna-rna-)  
410 [https://community.nanoporetech.com/technical\\_documents/minknow-tech-](https://community.nanoporetech.com/technical_documents/minknow-tech-)  
411 [doc/v/mitd\\_5000\\_v1\\_revaa\\_16may2016](https://community.nanoporetech.com/technical_documents/minknow-tech-)
- 412 6. Oxford Nanopore Technologies, Guppy basecaller tool (2020), <https://nanoporetech.com/>
- 413 7. Leger A, Leonardi T, pycoQC, interactive quality control for Oxford Nanopore Sequencing.  
414 *Journal of Open Source Software* (2019), 4(34), 1236, <https://doi.org/10.21105/joss.01236>
- 415 8. Wouter De Coster, Sven D'Hert, Darrin T Schultz, Marc Cruys, Christine Van Broeckhoven,  
416 NanoPack: visualizing and processing long-read sequencing data, *Bioinformatics*, Volume  
417 34, Issue 15, 01 August 2018, Pages 2666–2669,  
418 <https://doi.org/10.1093/bioinformatics/bty149>
- 419 9. Schneider VA, Graves-Lindsay T, Howe Kerstin et al., Evaluation of GRCh38 and de novo  
420 haploid genome assemblies demonstrates the enduring quality of the reference assembly,  
421 *bioRxiv* (2016), Cold Spring Harbor Laboratory, <https://doi.org/10.1101/072116>
- 422 10. Bethesda (MD): National Library of Medicine (US), National Center for Biotechnology  
423 Information, (1988) [cited 2020 Jun 28]. Available from: <https://www.ncbi.nlm.nih.gov/>
- 424 11. Bethesda (MD): National Library of Medicine (US), National Center for Biotechnology  
425 Information, (1988), Accession No. NC\_045512.2, Severe acute respiratory syndrome  
426 coronavirus 2 isolate Wuhan-Hu-1, complete genome; [cited 2020 Jun 28]. Available from:  
427 [https://www.ncbi.nlm.nih.gov/nuccore/NC\\_045512.2/](https://www.ncbi.nlm.nih.gov/nuccore/NC_045512.2/)
- 428 12. Li H, Minimap2: pairwise alignment for nucleotide sequences. *Bioinformatics* (2018), 34,  
429 3094-3100.
- 430 13. Lin, H., Hsu, W. GSAalign: an efficient sequence alignment tool for intra-species genomes.  
431 *BMC Genomics* 21, 182 (2020). <https://doi.org/10.1186/s12864-020-6569-1>
- 432 14. Li H, Handsaker B, Wysoker A, et al. 1000 Genome Project Data Processing Subgroup, The  
433 Sequence alignment/map (SAM) format and SAMtools, *Bioinformatics* (2009) 25(16) 2078-9
- 434 15. Li H, A statistical framework for SNP calling, mutation discovery, association mapping and  
435 population genetical parameter estimation from sequencing data, *Bioinformatics* (2011)  
436 27(21) 2987-2993.
- 437 16. James T. Robinson, Helga Thorvaldsdóttir, Aaron M. Wenger, Ahmet Zehir, Jill P. Mesirov.  
438 Variant Review with the Integrative Genomics Viewer (IGV). *Cancer Research* (2017),  
439 77(21) 31-34.
- 440 17. Vacca D, Cancila V, Gulino A, et al. Real-time detection of BRAF V600E mutation from  
441 archival hairy cell leukemia FFPE tissue by nanopore sequencing. *Mol Biol Rep.*  
442 2018;45(1):1-7. doi:10.1007/s11033-017-4133-0

- 443 18. Trost B, Walker S, Haider SA, et al. Impact of DNA source on genetic variant detection from  
444 human whole-genome sequencing data. *J Med Genet.* 2019;56(12):809-817.  
445 doi:10.1136/jmedgenet-2019-106281
- 446 19. Zhu Q, Hu Q, Shepherd L, et al. The impact of DNA input amount and DNA source on the  
447 performance of whole-exome sequencing in cancer epidemiology. *Cancer Epidemiol*  
448 *Biomarkers Prev.* 2015;24(8):1207-1213. doi:10.1158/1055-9965.EPI-15-0205
- 449 20. Shanker S, Paulson A, Edenberg HJ, et al. Evaluation of commercially available RNA  
450 amplification kits for RNA sequencing using very low input amounts of total RNA. *J Biomol*  
451 *Tech.* 2015;26(1):4-18. doi:10.7171/jbt.15-2601-001
- 452 21. Depledge DP, Wilson AC. Using Direct RNA Nanopore Sequencing to Deconvolute Viral  
453 Transcriptomes. *Curr Protoc Microbiol.* 2020;57(1):e99. doi:10.1002/cpmc.99
- 454 22. Zhao WM, Song SH, Chen ML, et al. The 2019 novel coronavirus resource. *Yi Chuan.*  
455 2020;42(2):212–221. doi:10.16288/j.ycz.20-030